(Received 17 April 2025, Accepted 12 June 2025, Scheduled 13 July 2025)

New Approach to Extract the Complex Relative Permittivity from Two Circular Coaxial Transmission Lines

Ghislain F. Bouesse[1, 2], Amour E. G. Langa-Etotsou[1, 2], and Franck Moukanda Mbango[2, 3, *]

[1] *Ecole Nationale Supérieure Polytechnique (ENSP), Université Marien Ngouabi, BP 69, Brazzaville, Republic of the Congo*
[2] *Laboratoire d'Electronique et d'Electrotechnique, Université Marien Ngouabi, BP 69, Brazzaville, Republic of the Congo*
[3] *Faculté des Sciences et Techniques (FST), Université Marien Ngouabi, BP 69, Brazzaville, Republic of the Congo*

ABSTRACT: This paper investigates a new, simple, fast, and broadband procedure to extract the material intrinsic parameters through new mathematical modeling. It only uses the transmission coefficient of two identical lines. The method is based on the mathematical reformulation of the two transmission lines, taking into account the effects of discontinuities at the interface connecting the trapper and the connector, as well as the included S-parameters. These test cells have different lengths, so the sample under test (SUT) complex relative permittivity is determined after fixing the vacuum structure's electric length. At the same time, the mathematical formulation of the telecommunications equation, which links transmission and reflection coefficients, was used to determine the loss tangent parameter by combining the attenuation and phase coefficients. The correction of the electric length difference of the transmission coefficients resulting from the measurement of the vacuum-filled test cells is done using an affine function. The frequency is the variable parameter, and the slope (rate of variation) and the initial value (ordered at the origin) are computed according to the test cell used. On the one hand, the suggested principle has the advantage of extracting the relative permittivity of the sample under test beyond the limit set by the appearance of higher-order modes (propagated by considering the test fixture's transverse dimensions). On the other hand, the use of the reflection coefficient, although it improves the attenuation coefficient extraction, limits the characterization band of the loss tangent. A circular coaxial test fixture has been used in the 1–20 GHz frequency range to validate the proposed method with samples of various materials, including semolina, polenta, Q-Cell 5020 (ceramic powder), aquarium stone, distilled water, and phantom gel. The results are compared with those from the two transmission lines technique, as defined in its popular form.

1. INTRODUCTION

Researchers and developers in industries face significant challenges when producing new transmission equipment or devices. Thus, users increasingly demand more compact gadgets that perform well. That is why, among the many possibilities that arise, we find the opportunity to utilize existing materials that are well known or to create new ones. All these offer more flexibility in designing and manufacturing new transmission devices. The ease of integration, low cost, and high performance of these devices require sound knowledge and control of materials. This can only be achieved by developing techniques (new or existing) that meet the requirements of the goals to be achieved [1]. The methods used are thus a set of processes employed to obtain a determined result. In this context, there are six major families: probe technology (applicators) [2, 3], free space [4–6], transmission lines (short-circuit, open circuit, etc.) [7], spiral or coils, parallel plate capacitors, and resonant cavity [8]. Several sets of reasoned approaches were followed to extract complex relative permittivity from the literature. These methods can be classified into two prominent families: narrowband or broadband, destructive or nondestructive [9], lumped or distributed elements, and resonant or nonresonant. The shape and state of the sample under test (SUT) require an adaptation of the sample holder to the frequency range to be scanned and the precision to be achieved from the parameter to be extracted [1]. Through the use of electrical (dielectric, semiconductor, conductor), magnetic (ferromagnetic, etc.) [10, 11], and magnetoelectric [12] materials, devices, such as filters [13], antennas [14], and oscillators [15], play a key role in various devices and appliances in improving the lives of consumers through more demanding specifications that suppliers and other industrialists must respect.

Although resonant cavity technique achieves the best precision on loss tangent and relative permittivity [16], it suffers from the narrowness of the bandwidth frequency to be scanned [17]. Thus, transmission lines become serious candidates due to the frequency range (broadband) to be covered [12]. In that case, transmission line technique became the most well-known technique [18, 19], especially two-line-line technique, because of the difference in the test cell lengths. One- or two-port transmission structures dedicated to wafers or liquids can be homogeneous or inhomogeneous [20]. The newly developed approaches consist of differences in the transmission coefficient phase constant $(\Delta\Phi_v)$ of both lengths in vacuum and SUT configurations. This new approach introduces an additional term when using the product of the chain scattering matrix. Moreover, the expression of the latest mathematical model creates a disturbance of the received signal in

* Corresponding author: Franck Moukanda Mbango (franck.moukandambango@umng.cg).

a small frequency range in the vacuum case. Hence the need to fix the defect becomes a necessity. Using the affine function [21] to correct some imperfections of $\Delta\Phi_v$ is a key point in broadening the frequency range of the study. The loss tangent is determined using the telecommunication principle through attenuation coefficient [22], which uses the reflection and transmission coefficients of the whole structure without the need for de-embedding step. The proposed approach is based solely on utilizing the transmission coefficient arguments of the two trap devices and telecommunication equation to calculate the attenuation coefficient, in both the absence and presence of the tested sample. This is aimed at achieving the primary goal of extracting the SUT's relative permittivity and loss tangent. Referring to [7], the authors use the characteristic impedances of the different line segments and a third-degree polynomial function. Some authors sometimes use second-degree or exponential polynomial functions to represent an extraction model of the complex permittivity of materials [23].

The two approaches adopted are easy to implement, quick to execute, reliable, and more precise regarding the results obtained. They cover an extensive frequency band compared to the conventional transmission line method. They better correct the discontinuity effects at contact interfaces between the connector and SUTs' trapper. Biofood materials (semolina, polenta), ceramic powders (Q-Cell 5020), biomass (distilled water, aquarium stone), and transmission gel for industrial, scientific, and medical (ISM) applications were used as test samples to validate the proposed new approach. An HP Agilent 8510C vector network analyzer (VNA) has been utilized as an radio frequency (RF) measurement device for experimental validation in the 1–20 GHz frequency range. This paper describes a novel approach to processing the two-line technique. Two main sections are dedicated to it: methodology and experimental validation. The study will conclude with a comparison of results with those available in the literature.

2. METHODOLOGY OF THE SUGGESTED APPROACHES

A transmission line comprises an ideal line, where the SUT is trapped, and two connectors at the ends [24]. These two connectors can be connected to the measuring device for S-parameters data acquisition.

The two connectors are generally considered identical when different approaches are developed. However, this is not necessarily the reality because of manufacturing risks. This assumption is often considered when approaching the difference in line lengths through the two transmission lines technique.

Figure 2 is the two-line-line method simplified representation, where two identical devices under test (DUT), which differ in physical lengths l_1 and l_2. Each DUT measurement should be taken with the device empty and then filled with the sample to be tested. The acquisition of data through S-parameters allows us to define the chain scattering matrix for each trapper before associating both and determining the equivalent chain scattering matrix. Due to the mathematical formulation, additional terms are observed. The measurement of a vacuum-filled sample trapper is a real challenge in the field of material characterization because it limits the frequency band to be covered. Thus, the proposed method addresses this limitation by incorporating an additional term for reflection elements into the classical formulation of the two-line transmission method. The results are compared with those obtained using the two-line method and the well-known conventional formulation.

2.1. The Two-Line-Line Technique: Popular Description

Two-transmission-line technique is one of the most popular methods, based on T-matrix (chain scattering matrix) or R-matrix (cascading matrix), to determine the equivalent propagation constant.

$$[R] = [T]^{-1} \tag{1}$$

That procedure partially solves the problem of contact interfaces between the connector and ideal trapper fixture [26]. The technique utilizes two identical fixtures with the exact cross-sectional dimensions but differing in their longitudinal dimensions (physical length $l_2 > l_1$). The chain scattering matrix is related to S-parameters of the fixture's two-port network [27] by,

$$\left[T_{1,2}^{v,m}\right] = \begin{bmatrix} T_{(11)_{1,2}}^{v,m} & T_{(12)_{1,2}}^{v,m} \\ T_{(21)_{1,2}}^{v,m} & T_{(22)_{1,2}}^{v,m} \end{bmatrix} = \frac{1}{S_{(21)_{1,2}}} \begin{bmatrix} 1 & -S_{(22)_{1,2}} \\ S_{(11)_{1,2}} & S_{(12)_{1,2}}S_{(21)_{1,2}} - S_{(11)_{1,2}}S_{(22)_{1,2}} \end{bmatrix} \tag{2}$$

where S_{11} and S_{21} are the reflection and transmission coefficients, respectively. Such a definition emphasizes the use of reflection and transmission coefficients. Subscript letters v and m symbolize the vacuum and sample under test while $[T_{1,2}]$ means T-matrix for the test cell of length l_1 and l_2, respectively. The following operation,

$$[T_{\Delta L}] = [T_2^{v,m}] \cdot [T_1^{v,m}]^{-1} = \begin{bmatrix} T_{(11)_{v;m}}^{(\Delta L)} & T_{(12)_{v,m}}^{(\Delta L)} \\ T_{(21)v,m}^{(\Delta L)} & T_{(22)v,m}^{(\Delta L)} \end{bmatrix} \tag{3}$$

allows determining the propagation constant $(\gamma\Delta L)$ of the ideal line after correcting discontinuities, which becomes,

$$\begin{cases} \gamma_{v,m}\Delta L = \cosh^{-1}\left\{\frac{T_{(11)_{v;m}}^{(\Delta L)} + T_{(22)_{v;m}}^{(\Delta L)}}{2}\right\} \\ \text{or} \\ \gamma_{v,m}\Delta L = \ln\left(\lambda_1^{v,m}\right) = -\ln\left(\lambda_2^{v,m}\right) \end{cases} \tag{4}$$

where the eigenvalues are,

$$\lambda_{1,2}^{v,m} = \frac{\left(T_{(11)_{v;m}}^{(\Delta L)} + T_{(22)_{v;m}}^{(\Delta L)}\right) \pm \sqrt{\left(T_{(11)_{v;m}}^{(\Delta L)} - T_{(22)_{v;m}}^{(\Delta L)}\right)^2 + 4T_{(12)_{v;m}}^{(\Delta L)} T_{(21)_{v;m}}^{(\Delta L)}}}{2} \tag{5}$$

The coaxial fixture used is homogeneous, then $\varepsilon^*_{eff} = \varepsilon^*_r$. In that case, the relative permittivity is obtained as,

$$\varepsilon'_r = \left(\frac{\Delta\theta_m}{\Delta\theta_v}\right)^2 \tag{6}$$

and the loss tangent becomes,

$$\tan\delta_d = 2\left\{\frac{\alpha_m \Delta L}{\Delta\theta_m} - \frac{\alpha_v \Delta L}{\Delta\theta_v}\right\} \tag{7}$$

where,

$$\begin{cases} \gamma_{v,m}\Delta L = \alpha_{v,m}\Delta L + j\theta_{v,m} \\ \Delta L = l_2 - l_1 \end{cases} \tag{8}$$

This formulation does not consider the effects of the discontinuity circuit at the junction connector and trap line, in which case, the result would not be as quoted in several publications [28]. Hence, revisiting the mathematical formulation becomes both a challenge and an imperative.

2.2. The Two-Line-Line Technique: New Mathematical Model

As demonstrated by the previous equations, this two-line technique emphasizes the use of reflection coefficients. This has a significant impact, especially on the phase extracted when measuring the vacuum-filled test cell. Let us consider the following definition,

$$[T] = \begin{cases} [T_1] = \underbrace{\begin{bmatrix} e^{\gamma_0 l_0} & 0 \\ 0 & e^{-\gamma_0 l_0} \end{bmatrix}}_{[X]} \underbrace{\begin{bmatrix} (1-\Gamma)^{-1} & \Gamma(1-\Gamma)^{-1} \\ \Gamma(1-\Gamma)^{-1} & (1-\Gamma)^{-1} \end{bmatrix}}_{[\Gamma_D]} [T_{l_1}] \underbrace{\begin{bmatrix} (1-\Gamma)^{-1} & \Gamma(1-\Gamma)^{-1} \\ \Gamma(1-\Gamma)^{-1} & (1-\Gamma)^{-1} \end{bmatrix}}_{[\Gamma_D]} \underbrace{\begin{bmatrix} e^{\gamma_0 l_0} & 0 \\ 0 & e^{-\gamma_0 l_0} \end{bmatrix}}_{[X]} \\ [T_2] = \underbrace{\begin{bmatrix} e^{\gamma_0 l_0} & 0 \\ 0 & e^{-\gamma_0 l_0} \end{bmatrix}}_{[X]} \underbrace{\begin{bmatrix} (1-\Gamma)^{-1} & \Gamma(1-\Gamma)^{-1} \\ \Gamma(1-\Gamma)^{-1} & (1-\Gamma)^{-1} \end{bmatrix}}_{[\Gamma_D]} [T_{l_2}] \underbrace{\begin{bmatrix} (1-\Gamma)^{-1} & \Gamma(1-\Gamma)^{-1} \\ \Gamma(1-\Gamma)^{-1} & (1-\Gamma)^{-1} \end{bmatrix}}_{[\Gamma_D]} \underbrace{\begin{bmatrix} e^{\gamma_0 l_0} & 0 \\ 0 & e^{-\gamma_0 l_0} \end{bmatrix}}_{[X]} \end{cases} \tag{9}$$

Rewriting Equation (3) leads to,

$$[T_{\Delta L}] = [X]\,[\Gamma_D]\,\underbrace{\left[T^{v,m}_{l_2}\right]\left[T^{v,m}_{l_1}\right]^{-1}}_{\left[T^{v,m}_{\Delta l}\right]}\,[\Gamma_D]^{-1}\,[X]^{-1} \tag{10}$$

Solving Equation (10) leads to a matrix with three unknown parameters: Γ (the reflection coefficient at the interface connector — trapper), $\gamma_0 l_0$ (the connector's propagation constant), and $\gamma\Delta l$. The true matrix representing the discontinuity correction's principle is given as follows,

$$\left[T^{v,m}_{\Delta l}\right] = \left[T^{v,m}_{l_2}\right]\left[T^{v,m}_{l_1}\right]^{-1} \tag{11}$$

and

$$[T_{\Delta L}] = \frac{1}{(1-\Gamma^2)} \begin{bmatrix} (e^{\gamma\Delta l} - \Gamma^2 e^{-\gamma\Delta l}) & \Gamma(e^{-\gamma\Delta l} - e^{\gamma\Delta l})e^{2\gamma_0 l_0} \\ \Gamma(e^{\gamma\Delta l} - e^{-\gamma\Delta l})e^{-2\gamma_0 l_0} & (e^{-\gamma\Delta l} - \Gamma^2 e^{\gamma\Delta l}) \end{bmatrix} = \begin{bmatrix} T^{11}_{\Delta l} & T^{12}_{\Delta l} \\ T^{21}_{\Delta l} & T^{22}_{\Delta l} \end{bmatrix} \tag{12}$$

Solving Equation (12), it is possible to determine the connector's propagation constant as defined below,

$$\gamma_0 l_0 = \frac{1}{2}\ln\left(-\frac{T^{12}_{\Delta l}}{T^{21}_{\Delta l}}\right) \tag{13}$$

This result is particularly interesting when the DUT is filled with a vacuum. Let us consider Equation (3) and express $[T_{\Delta L}]$ with S-parameters,

$$[T_{\Delta L}] = \frac{1}{S^{(l_1)}_{21} S^{(l_2)}_{21}} \begin{bmatrix} \left(S^{(l_2)}_{22} S^{(l_1)}_{11} - \Delta S^{(l_1)}\right) & \left(S^{(l_1)}_{22} - S^{(l_2)}_{22}\right) \\ \left(S^{(l_1)}_{11}\Delta S^{(l_2)} - S^{(l_2)}_{11}\Delta S^{(l_1)}\right) & \left(S^{(l_2)}_{11} S^{(l_1)}_{22} - \Delta S^{(l_2)}\right) \end{bmatrix} \tag{14}$$

as well as,

$$T^{11}_{\Delta l} + T^{22}_{\Delta l} = 2\left(\frac{S^{(l_2)}_{21} S^{(l_2)}_{12} + S^{(l_1)}_{21} S^{(l_1)}_{12}}{2S^{(l_1)}_{21} S^{(l_2)}_{21}}\right) + \Psi(S) \tag{15}$$

where,

$$\gamma\Delta l = \cosh^{-1}\left\{\frac{S^{(l_2)}_{21} S^{(l_2)}_{12} + S^{(l_1)}_{21} S^{(l_1)}_{12}}{2S^{(l_1)}_{21} S^{(l_2)}_{21}}\right\} \tag{16}$$

and,

$$\Psi(S) = \frac{S^{(l_2)}_{11}\left(S^{(l_1)}_{22} - S^{(l_2)}_{22}\right) + S^{(l_1)}_{11}\left(S^{(l_2)}_{22} - S^{(l_1)}_{22}\right)}{S^{(l_2)}_{21} S^{(l_1)}_{21}} \tag{17}$$

Based on the mathematical model presented in Equation (9), the reflection coefficients, as shown in Equations (12) and (14), and those that follow, do not allow for the precise definition of

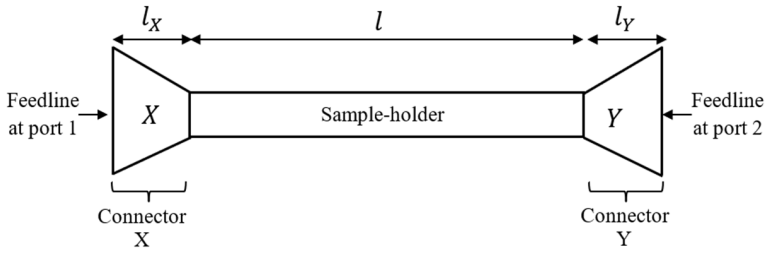

FIGURE 1. A transmission line with all its elements.

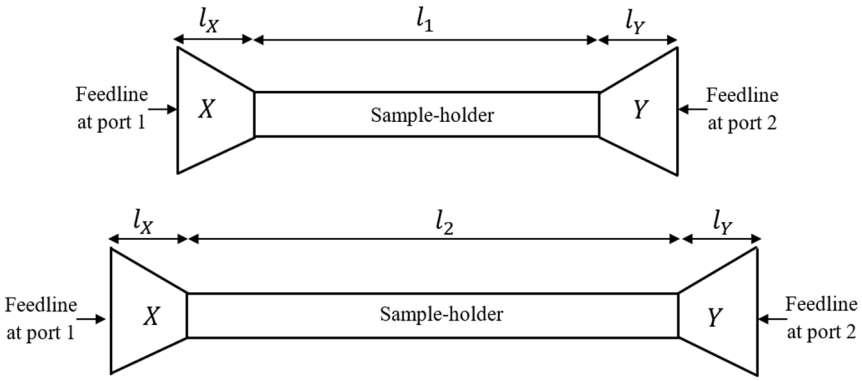

FIGURE 2. Reduced model of the line-line method trapping a SUT [25].

the deviation of the sought propagation constant. Equation (15) demonstrates that the approximation made through the condition presented by Equation (4) is a limiting factor of the frequency band in determining the propagation constant of the line segment devoid of discontinuities. Hence, Equation (18) only considers the transmission effects by removing the additional term that limits the frequency band to be covered. Equation (17) appears as an additional term, which reduces the study frequency band. This extra term can be associated with the one showing the effects of discontinuities from a cut-off frequency. Using the reasoning developed by several researchers who have worked around the problem of transmission lines, we can establish that the choice of function is essential. Indeed, the hyperbolic cosine function is prone to not providing the same level of precision across different data processing software. In that case, it appears that,

$$\gamma \Delta l = \ln\left\{\frac{S_{12}^{(l_2)}}{S_{21}^{(l_1)}}\right\} = -\ln\left\{\frac{S_{12}^{(l_1)}}{S_{21}^{(l_2)}}\right\} \tag{18}$$

The cut-off frequency is closely related to the sample holder's cross-sectional dimensions and intrinsic parameters of the SUT. Using the trigonometric function, such as hyperbolic cosines, may generate numerical errors that must be corrected. Therefore, it is suggested to use the logarithmic function as given in Equation (18).

2.3. The Two Line-Line Technique: Quick Resolution Approach

Due to the imperfections at the contact interference, the mathematical methodology is presented in this sub-section to avoid the de-embedding operation through the matrix computation. Reflection (S_{11}) and transmission (S_{21}) coefficients [29] are data from the VNA due to the disturbance of electric and magnetic field lines within the test cell [30, 31]. On one hand, the combination of these two parameters allows us to determine the attenuation coefficient [22] as given below,

$$\alpha^{v,m} l = \frac{1}{20\log(e)} \left\{-S_{21_{(v,m)}}^{dB} + S_{11_{(v,m)}}^{dB} + 10\log\left\{\frac{1}{|S_{11}|^2} - 1\right\}\right\} \tag{19}$$

where (αl) is expressed in neper (Np). This equation combines the transmission and reflection coefficients, allowing for the solution of resonances closely related to the physical length of the test cell and the various materials present. On the other hand, the phase of the transmission coefficient is deduced from Euler's theorem by the equation given as follows,

$$\theta_{1,2}^{v,m} = -j\left\{\ln\left(\frac{S_{21}^{v,m}}{|S_{21}^{v,m}|}\right)\right\} \tag{20}$$

The attenuation coefficient is calculated through Equation (18). The metal bloc and open-coaxial probe, as shown in Figure 1, are different elements of the test cell used for the suggested approach. The propagation speed is not frequency-dependent when a transverse electromagnetic or quasi-TEM mode propagates. Thus, phase jumps do not exist. Hence, there is a need to linearize the phase, which can oscillate between π and $-\pi$.

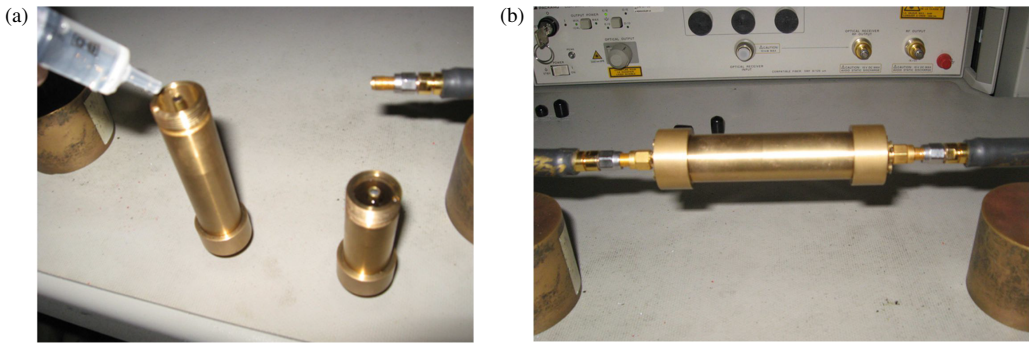

FIGURE 3. (a) Filling of the two identical trappers with distilled water. (b) Radio frequency measurement bench with the device under test for S-parameters' data acquisition.

$\Phi_{1,2}^{v,m}$ denotes the linearized phase and $\Delta\Phi_{v,m}$ the difference between these phases, such as,

$$\begin{cases} \Delta\Phi_m = \Phi_2^m - \Phi_1^m \\ \Delta\Phi_v = \Phi_2^v - \Phi_1^v \end{cases} \tag{21}$$

By referring to Equation (6), it is deduced that the relative permittivity [32] of the SUT in its new definition becomes,

$$\varepsilon'_{r_{(ND)}} = \left(\frac{\Delta\Phi_m}{\Delta\Phi_v}\right)^2 = \left(\frac{\Phi_2^m - \Phi_1^m}{\Phi_2^v - \Phi_1^v}\right)^2 \tag{22}$$

This formulation enables the correction of defects in connectors, whether identical or not, as well as the effects of discontinuities, particularly when the sample holder is filled with SUT. Thus, the affine functions approach [33] improves the acquired phase when the test cell is filled with vacuum (i.e., an environment without charges). The form of the function is,

$$\Delta\Phi_c^v(f) = Af + B \tag{23}$$

where the rate of variation "A" and the initial value "B" are given as follows [34],

$$A = \frac{\Delta\Phi_n^v - \Delta\Phi_k^v}{f_n - f_k} \tag{24}$$

and,

$$B = \frac{\Delta\Phi_k^v f_n - \Delta\Phi_n^v f_k}{f_n - f_k} \tag{25}$$

The needed function is written as presented in the equation below,

$$\Delta\Phi_c^v(f) = \left(\frac{1}{f_n - f_k}\right) \{(\Delta\Phi_n - \Delta\Phi_k) f + (\Delta\Phi_k f_n - \Delta\Phi_n f_k)\} \tag{26}$$

This new formulation $\Delta\Phi_c^v$ results in a novel approach to the rapid extraction of the relative permittivity of the SUT.

$$\varepsilon'_{r_{(NF)}} = \left(\frac{\Phi_2^m - \Phi_1^m}{\Delta\Phi_c^v}\right)^2 \tag{27}$$

Finally, it is observed that Equation (16) is in scientific conformity with Equations (19) and (21). Further investigations will be made using the following experimental measures to validate this assertion. Using Equations (19), (21), and (26), the dielectric loss tangent can be determined as given in Equation (28) below,

$$\tan\delta_{d_{(NF)}} = 2\left\{\frac{\left(\alpha_m^{(l_2)} - \alpha_m^{(l_1)}\right)\Delta L}{\Delta\Phi_m} - \frac{\left(\alpha_v^{(l_2)} - \alpha_v^{(l_1)}\right)\Delta L}{\Delta\Phi_c^v}\right\} \tag{28}$$

The electric lengths "θ" and "Φ" are related to the phase constant "β" and physical length "l" in the relation below [35],

$$\theta = \beta l \tag{29}$$

These electrical lengths are linearized [36, 37] to correct the observed phase breaks.

3. MEASUREMENT RESULTS AND DISCUSSION

A circular coaxial test cell has been manufactured, as shown in Figure 3, to validate the new definition of the two-transmission line technique (TTLT). The test cell has an inner-outer conductor diameter of $D = 14.36$ mm. In comparison, the outer-inner conductor is $d = 4$ mm. Both test cells have lengths of 63.60 mm and 83.60 mm.

The HP Agilent 8510C vector network analyzer (VNA) utilizes RF technology. This kind of RF equipment is often used in this domain [38]. This equipment enables broadband measurements from 45 MHz to 50 GHz using a 2.4 mm coaxial kit calibration. Thus, after having filled the vacuum trap or test sample, as presented in Figure 3(a), it is inserted and connected to the RF measurement equipment for S-parameters data acquisition. This is shown in Figure 3(b). Imported on a data processing software and taking into account the two chosen mathematical models (popular formulation and novelty proposed model), a program is written. The well-known model serves as a reference basis for comparing results from the stated formulation. This comparison provides a solid basis for supporting the proposed model choice. The principle of filling sample carriers with the SUT remains the same while considering the SUT state and shape. The samples tested are the Q-Cell 5020, fine po-

TABLE 1. The extracted values of phantom gel at 900 MHz.

Parameter/Technology	Manufacturer	Suggested formulation
Relative permittivity ε'_r	$41.4 \pm 5\%$	41.194
Electric conductivity σ (S/m)	0.95	0.965
Method	Resonant cavity	Transmission line

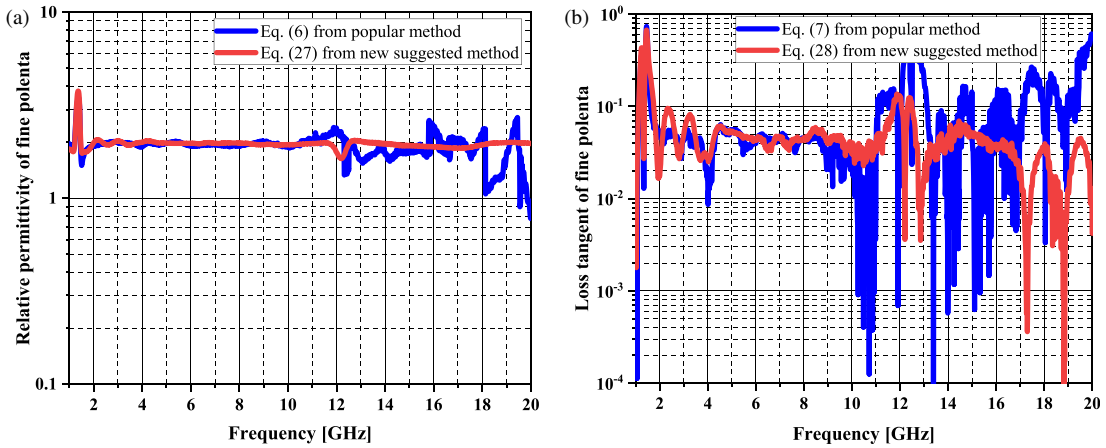

FIGURE 4. (a) Scanned frequency of the fine polenta's relative permittivity. (b) Scanned frequency of the fine polenta's loss tangent.

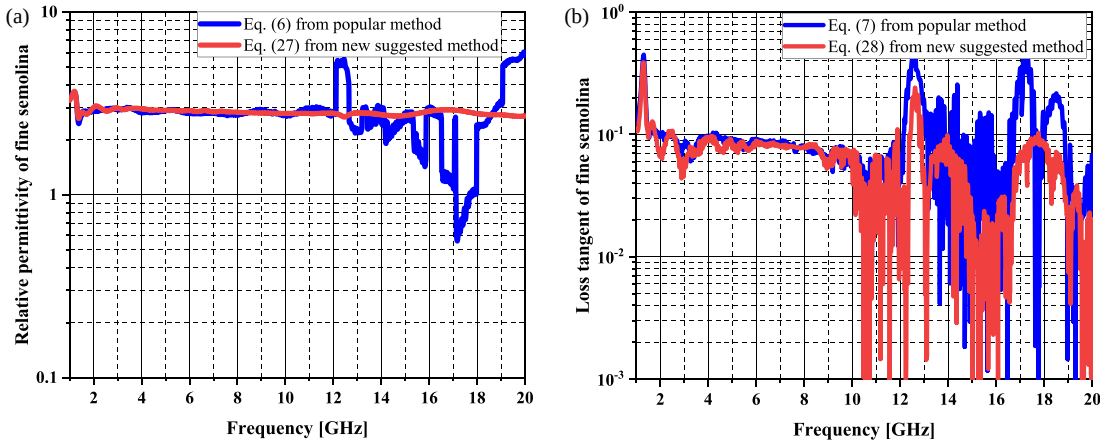

FIGURE 5. (a) Scanned frequency of the fine semolina's relative permittivity. (b) Scanned frequency of the fine semolina's loss tangent.

lenta, fine semolina, aquarium stone, distilled water, and phantom gel [39].

The suggested new formulation aligns perfectly with the results observed in Figures 4, 5, 6, 7, and 8. Also, they show a promising trend in the curves from different formulations. The results, presented in various figures, are compared with those obtained using the line-line method, which employs a different mathematical formulation, as illustrated in these figures.

Apart from the perfect agreement of the trend among all results, we can also raise the frequency band's size. These results prove that using approximations through affine functions is a well-adapted principle in material characterization [40], especially in the case of vacuum. Indeed, all samples tested, whose extraction model is based on Equation (18), show results in a broader frequency range. It is worth noting that the test cells and measurements are conducted under the same conditions. In other words, the processing data is the same.

The phantom gel is a transmittance substance for medical imaging applications. It is also known as Liquid 900 MHz, and the manufacturer employed the resonant cavity method to obtain results at 900 MHz. Table 1 summarizes the comparison of extracted values between the suggested method and those provided by the supplier ANTENESSA.

On the one hand, the differences between the extracted values are not as significant. This shows the reliability of the proposed formulation. On the other hand, it is noticed that the frequency band covered by the study using the new formulation is almost double. This is a significant benefit. The literature is rich in the electrical parameters of pure or distilled water; a comparative study is presented in Table 2. According to this

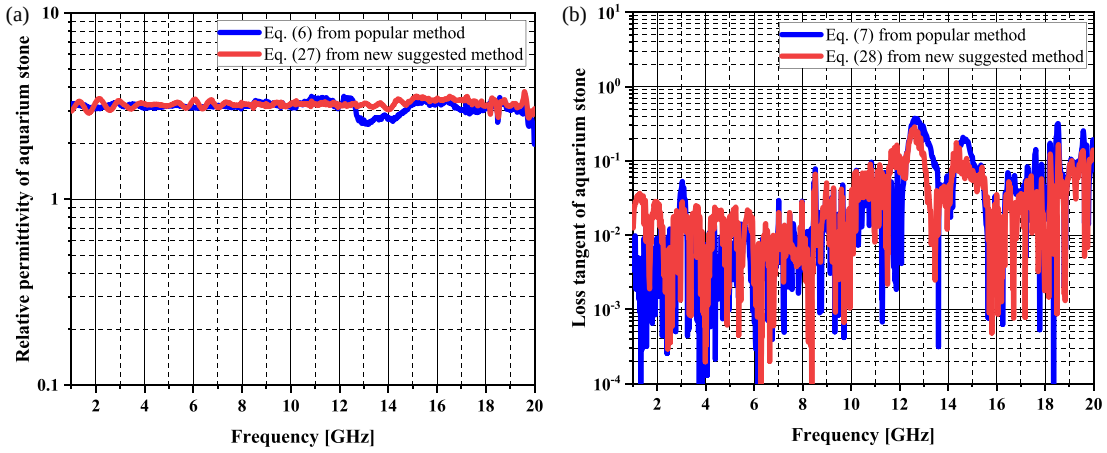

FIGURE 6. (a) Scanned frequency of the aquarium stone relative permittivity. (b) Scanned frequency of the aquarium stone's loss tangent.

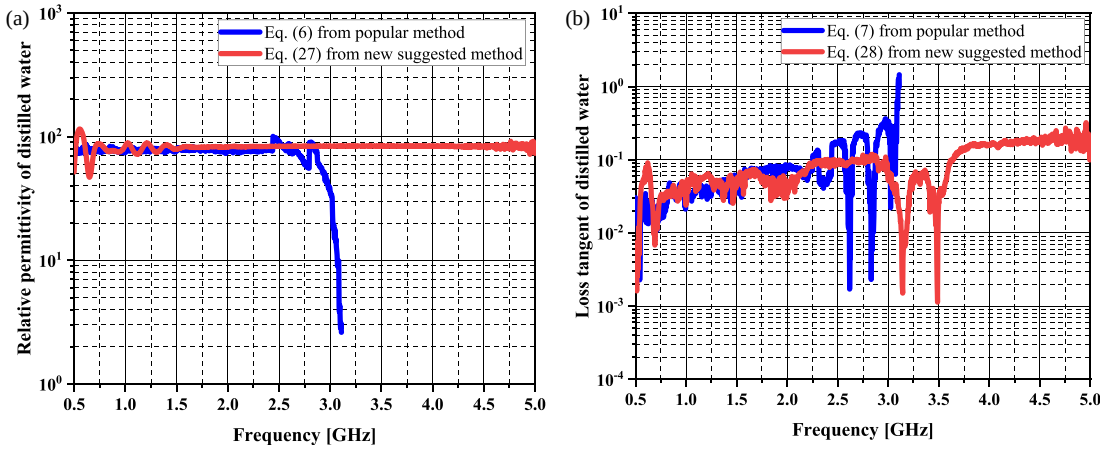

FIGURE 7. (a) Scanned frequency of the distilled water relative permittivity. (b) Scanned frequency of the distilled water loss tangent.

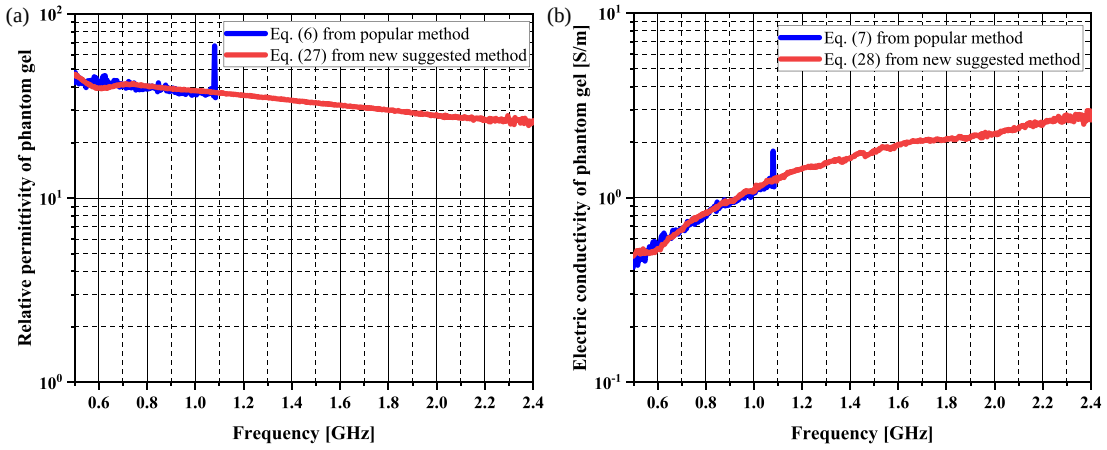

FIGURE 8. (a) Scanned frequency of phantom gel (Liquid 900 MHz) relative permittivity. (b) Scanned frequency of phantom gel (Liquid 900 MHz) electric conductivity.

claim, the relative permittivity of pure water is approximately 80 [41].

The proposed approach uses only the correction of electrical length defects in the case of a reference environment (empty), as its relative permittivity is always equal to one. This results in the non-adaptation of this approach to materials whose relative permittivity is very close to that of vacuum. Figure 9 shows the perfect illustration of this case.

For SUTs (see Figures 4–9), their behavior suggests that using the new formulation enables the extension of the frequency band, yielding results with improved accuracy. The results of the new approach are obtained with an error of less than 6%.

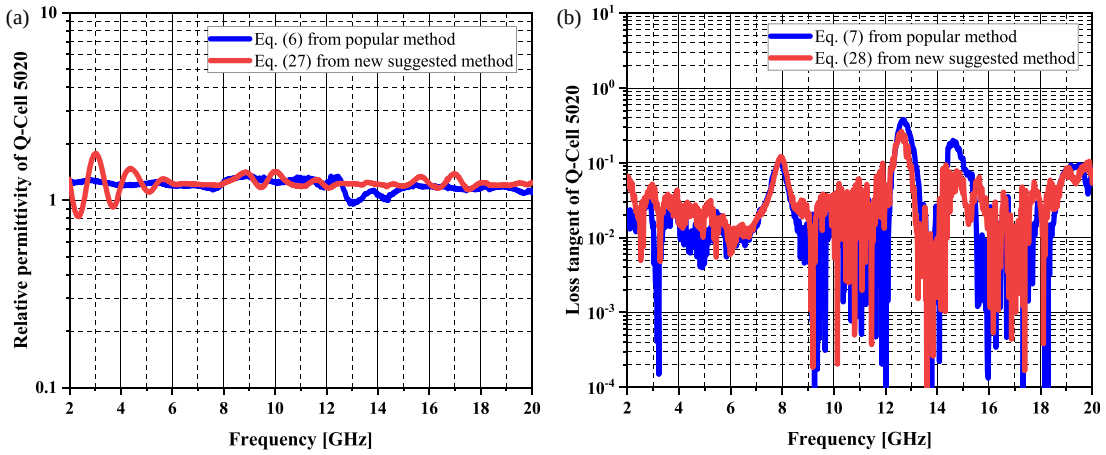

FIGURE 9. (a) Scanned frequency of the Q-Cell 5020 relative permittivity. (b) Scanned frequency of the Q-Cell 5020 loss tangent.

TABLE 2. Method's comparison of the extracted distilled water at 20°C.

Reference	Applied method	Relative permittivity ε'_r
[23]	Not provided	80.29
[42]	Capacitive sensor	80.00
Our work	Popular line-line formulation	79.257
	New line-line formulation	81.50

Figure 9 shows the difficulty of using this new extraction formulation for materials whose relative permittivity is close to one in the band below 5 GHz (in this case). This difficulty is mainly related to the ripples that appear in this frequency range. It can be assumed that the state of the contact interface between the connector and the trapper would cause the successive ripples observed during measurements of the empty test cells. From the overall view results, the developed approach demonstrates its reliability. It is better suited to high-k materials and applicable to high frequencies to avoid the effects leading to ripples, as shown in all results. Therefore, this new model offers good accuracy in a wide frequency band.

4. CONCLUSIONS

This paper uses two-transmission line technique to describe a new approach based on the latest mathematical model. A fixation on the fault resolution of the electrical length is made via an affine-type function for the vacuum case. The difference in this new approach is that it addresses ripples that appear in certain places. Two methods have been proposed for the same result in this paper: The difference in the propagation constant from each measured test cell's transmission coefficient and the multiplication of the chain scattering matrix remove the additional term that limits the frequency band to be covered. The goal is achieved by extending the covered frequency band compared to the conventional formula while increasing the accuracy of the extracted parameters. Two circular coaxial test cells have been manufactured, and the measurement bench is also equipped with an HP Agilent 8510C Vector Network Analyzer (VNA), which covers frequencies ranging from 1 to 20 GHz. Moreover, the experimental validation was conducted using five specimens: fine polenta, fine semolina, aquarium stone, Q-Cell 5020, and spring water. These sample holders have cross-sectional dimensions ($d = 4$ mm, $D = 14.36$ mm) and longitudinal dimensions ($l_1 = 63.60$ mm and $l_2 = 83.60$ mm). The new method demonstrated its broadband capability with an error of less than $\pm 6\%$ on relative permittivity across the entire frequency range of 1–20 GHz, according to the SUT. Low-k (polenta, semolina, aquarium stone, and Q-Cell 5020) and High-k (distilled water and Liquid 900 MHz) are tested insulators. In that case, the scanned frequency range depends on the SUT relative permittivity value.

ACKNOWLEDGEMENT

The authors thank the reviewers for their excellent contributions, which included relevant criticisms that helped strengthen this work. In addition, we would like to express our grateful acknowledgment to those from the Phénomène Electromagnétiques et Interactions avec l'Environnement (Phéline) platform for their multifaceted support during data acquisition, which enabled us to validate the work presented in this paper.

REFERENCES

[1] Bouesse, G. F. and F. Moukanda Mbango, "Probe with a metallic bowl termination to determine the electric material parameters from variable thicknesses," *Engineering Research Express*, Vol. 6, No. 1, 015314, 2024.

[2] Canicattì, E., N. Fontana, S. Barmada, and A. Monorchio, "Open-ended coaxial probe for effective reconstruction of biopsy-excised tissues' dielectric properties," *Sensors*, Vol. 24, No. 7, 2160, 2024.

[3] Fan, B., F. Bosc, Y. Liu, M. L. Feuvre, and C. Fauchard, "Permittivity analysis of weathered concrete in a bridge based on open-ended probe and impedance measurements," *Construction and Building Materials*, Vol. 429, 136354, May 2024.

[4] Diepolder, A., M. Mueh, S. Brandl, P. Hinz, C. Waldschmidt, and C. Damm, "A novel rotation-based standardless calibration and characterization technique for free-space measurements of dielectric material," *IEEE Journal of Microwaves*, Vol. 4, No. 1, 56–68, 2024.

[5] Ali, S. Z., K. Ahsan, D. ul Khairi, W. Alhalabi, and M. S. Anwar, "Advancements in FR4 dielectric analysis: Free space approach and measurement validation," *PLoS One*, Vol. 19, No. 9, e0305614, 2024.

[6] Xue, B., "Characterizing complex permittivity of thin materials by free space transmission and reflection coefficients," *IEEE Antennas and Wireless Propagation Letters*, Vol. 23, No. 12, 4438–4442, 2024.

[7] Moukanda Mbango, F., G. F. Bouesse, and F. Ndagijimana, "Extraction of the complex relative permittivity from the characteristic impedance of transmission line by resolving discontinuities," *Electronics*, Vol. 11, No. 23, 4035, 2022.

[8] Yamaguchi, T., N. Yamamoto, D. Naito, T. Takahashi, and S. Sakanaka, "Resonant cavity method based on RF measurement and simulation for measuring complex permittivity or permeability of RF absorbing materials," *Nuclear Instruments and Methods in Physics Research Section A: Accelerators, Spectrometers, Detectors and Associated Equipment*, Vol. 1064, 169449, 2024.

[9] Wang, J., E. G. Lim, M. P. Leach, Z. Wang, and K. L. Man, "Open-ended coaxial cable selection for measurement of liquid dielectric properties via the reflection method," *Mathematical Problems in Engineering*, Vol. 2020, No. 1, 8942096, 2020.

[10] Victoria, J., A. Suarez, P. A. Martinez, A. Amaro, A. Alcarria, J. Torres, R. Herraiz, V. Solera, V. Martinez, and R. Garcia-Olcina, "Advanced characterization of a hybrid shielding solution for reducing electromagnetic interferences at board level," *Electronics*, Vol. 13, No. 3, 598, 2024.

[11] Costa, F., M. Borgese, M. Degiorgi, and A. Monorchio, "Electromagnetic characterisation of materials by using transmission/reflection (T/R) devices," *Electronics*, Vol. 6, No. 4, 95, 2017.

[12] Lara, L. A., D. L. Mancipe, Y. Pineda, J. J. Moreno, and G. Peña-Rodríguez, "Design and characterization of a magneto-dielectric composite in high frequency with aligned magnetite powders," *Journal of Physics: Conference Series*, Vol. 1386, No. 1, 012103, 2019.

[13] Massamba, O. C., F. Moukanda Mbango, and D. Lilonga-Boyenga, "Four subbands from dual mismatched wideband bandpass filter for 5G/WAS/Wi-Fi/WiMAX/WLAN applications," *International Journal of RF and Microwave Computer-Aided Engineering*, Vol. 2023, No. 1, 4713995, 2023.

[14] Moukala Mpele, P., F. Moukanda Mbango, and D. B. O. Konditi, "Comparative analysis of five planar monopole antennas for LTE/C-V2X/5G/WiMAX applications," *Arabian Journal for Science and Engineering*, Vol. 48, No. 5, 6841–6855, 2023.

[15] Pikovsky, A. and F. Bagnoli, "Dynamics of oscillator populations with disorder in the coupling phase shifts," *New Journal of Physics*, Vol. 26, No. 2, 023054, 2024.

[16] Kombolias, M., J. Obrzut, M. T. Postek, D. L. Poster, and Y. S. Obeng, "Method development for contactless resonant cavity dielectric spectroscopic studies of cellulosic paper," *Journal of Visualized Experiments*, No. 152, e59991, 2019.

[17] Paul, R. B., A. E. Engin, and J. Aguirre, "Dielectric and underfill characterization using cavity resonators for millimeter-wave applications," *IEEE Letters on Electromagnetic Compatibility Practice and Applications*, Vol. 2, No. 3, 76–80, 2020.

[18] Farhat, I., L. Farrugia, J. Bonello, R. Grima, R. Persico, and C. Sammut, "One-port coaxial line sample holder characterisation method of dielectric spectra," *Sensors*, Vol. 24, No. 17, 5573, 2024.

[19] Zhang, J., M. Koledintseva, G. Antonini, J. Drewniak, A. Orlandi, and K. Rozanov, "Planar transmission line method for characterization of printed circuit board dielectrics," *Progress In Electromagnetics Research*, Vol. 102, 267–286, 2010.

[20] Moukanda Mbango, F., G. F. Bouesse, and F. Ndagijimana, "Material relative permittivity determination from the inhomogeneous transmission-line secondary parameters," *IEEE Access*, Vol. 10, 124 595–124 603, 2022.

[21] García-García, J. I., D. Marín-Aragón, A. Sánchez-Loureiro, and A. Vigneron-Tenorio, "Some properties of affine C-semigroups," *Results in Mathematics*, Vol. 79, No. 2, 52, 2024.

[22] Massamba, O. C., P. Moukala Mpele, F. Moukanda Mbango, and D. Lilonga-Boyenga, "Tri-band bandpass filter using mixed short/open circuited stubs and Q-factor with controllable bandwidth for WAS, ISM, and 5G applications," *Progress In Electromagnetics Research C*, Vol. 119, 177–190, 2022.

[23] Andryieuski, A., S. M. Kuznetsova, S. V. Zhukovsky, Y. S. Kivshar, and A. V. Lavrinenko, "Water: Promising opportunities for tunable all-dielectric electromagnetic metamaterials," *Scientific Reports*, Vol. 5, No. 1, 13535, 2015.

[24] Park, M.-S., J. Cho, S. Lee, Y. Kwon, and K.-Y. Jung, "New measurement technique for complex permittivity in millimeter-wave band using simple rectangular waveguide adapters," *Journal of Electromagnetic Engineering and Science*, Vol. 22, No. 6, 616–621, 2022.

[25] Moukanda Mbango, F., M. G. Lountala, E. J. D. M'Pemba, F. Ndagijimana, D. Lilonga-Boyenga, and B. M'Passi-Mabiala, "Comparison of materials characterization methods using one-port and two-port transmission line principles," *Int. J. Eng. Appl.*, Vol. 9, No. 6, 370–381, 2021.

[26] Zhang, Z., J. Liu, X. Xie, T. Hu, and S. Liu, "Data and model-driven 3D modeling method for transmission line LiDAR data," *Journal of Spatial Science*, Vol. 70, No. 2, 309–328, Dec. 2024.

[27] Edwards, T. C. and M. B. Steer, *Foundations for Microstrip Circuit Design*, 4th ed., 688, John Wiley & Sons, 2016.

[28] Reynoso-Hernandez, J. A., "Unified method for determining the complex propagation constant of reflecting and nonreflecting transmission lines," *IEEE Microwave and Wireless Components Letters*, Vol. 13, No. 8, 351–353, 2003.

[29] Ramos Somolinos, D., D. R. Somolinos, J. C. Estévez, B. P. Gallardo, C. P. Moravec, *et al.*, "Novel electromagnetic characterization methods for new materials and structures in aerospace platforms," *Materials*, Vol. 15, No. 15, 5128, 2022.

[30] Al-Nedawe, B. M., I. H. Ali, A. M. Ahmed, and H. M. Mahan, "Reflection and transmission coefficients measurements for polymer composites with a nano-PZT material using a non-resonant method," *IOP Conference Series: Materials Science and Engineering*, Vol. 1076, No. 1, 012065, 2021.

[31] Kim, S. and J. R. Guerrieri, "Low-loss complex permittivity and permeability determination in transmission/reflection measurements with time-domain smoothing," *Progress In Electromagnetics Research M*, Vol. 44, 69–79, 2015.

[32] Xiong, R., Y. Hu, A. Xia, K. Huang, L. Yan, and Q. Chen, "A high-temperature and wide-permittivity range measurement system based on ridge waveguide," *Sensors*, Vol. 25, No. 2, 541,

2025.

[33] Meuel, H. and J. Ostermann, "Analysis of affine motion-compensated prediction in video coding," *IEEE Transactions on Image Processing*, Vol. 29, 7359–7374, 2020.

[34] Dubuc, S., "Non-differentiability and Hölder properties of self-affine functions," *Expositiones Mathematicae*, Vol. 36, No. 2, 119–142, 2018.

[35] Sridhar, S. and Q. Li, "Multiphase constant on-time control with phase overlapping — Part I: Small-signal model," *IEEE Transactions on Power Electronics*, Vol. 39, No. 6, 6703–6720, Jun. 2024.

[36] Lin, B., S.-P. Li, Z.-C. Cao, Y. Zhang, and X.-M. Jiang, "Theoretical modeling and experimental analysis of single-grain scratching mechanism of fused quartz glass," *Journal of Materials Processing Technology*, Vol. 293, 117090, 2021.

[37] M'Pemba, J. E. D., G. F. Bouesse, F. Moukanda Mbango, and B. M'Passi-Mabiala, "Probes in transmission with material variable thicknesses to extract the material complex relative permittivity in 1.7–3 GHz," *Measurement: Sensors*, Vol. 20-21, 100369, 2022.

[38] Farcich, N. J., J. Salonen, and P. M. Asbeck, "Single-length method used to determine the dielectric constant of polydimethylsiloxane," *IEEE Transactions on Microwave Theory and Techniques*, Vol. 56, No. 12, 2963–2971, 2008.

[39] Bidgoli, H. A., N. Schieda, and C. Rossa, "A simplified formulation of the reflection coefficient of an open-ended coaxial probe in multilayered media," *IEEE Transactions on Microwave Theory and Techniques*, Vol. 72, No. 11, 6485–6495, 2024.

[40] Hasar, U. C., "Permittivity measurement of thin dielectric materials from reflection-only measurements using one-port vector network analyzers," *Progress In Electromagnetics Research*, Vol. 95, 365–380, 2009.

[41] Kolb, J., Y. Minamitani, S. Xiao, X. Lu, M. Laroussi, R. P. Joshi, K. H. Schoenbach, E. Schamiloglu, and J. Gaudet, "The permittivity of water under high dielectric stress," in *2005 IEEE Pulsed Power Conference*, 1266–1269, Monterey, CA, USA, Jun. 2005.

[42] Behzadi, G. and L. Fekri, "Electrical parameter and permittivity measurement of water samples using the capacitive sensor," *International Journal of Water Resources and Environmental Sciences*, Vol. 2, No. 3, 66–75, 2013.